Morphological Aspects of Rubber Fracture and Wear

D. M. Bieliński,[1,2] O. Dobrowolski,[1] G. Przybytniak[3]

[1]Institute of Polymer and Dye Technology, Faculty of Chemistry, Technical University of Łódź, Łódź, Poland
[2]Institute for Engineering of Polymer Materials and Dyes, Division of Elastomers and Rubber Technology, Piastów, Poland
[3]Department of Radiation Chemistry and Technology, Institute of Nuclear Chemistry and Technology, Warsaw, Poland

ABSTRACT: Morphology of carbon black (CB)-filled rubber was studied with AFM and SEM and the classification of filler agglomerates, based on their internal structure and filler–matrix interactions, has been proposed. It varies according to the activity of CB and the kind of rubber. It has been shown that fracture of rubber starts either inside filler agglomerates (de-cohesion) or in a filler–matrix interphase (de-adhesion) initiating wear of the material. Microscopic observations correlate well with TGA and EPR data of wear debris collected during friction of rubber. The increase of thermal stability of CB and the appearance of additional spin signals, respectively, for elongated samples or debris, are proposed to be associated with de-cohesion or de-adhesion of the agglomerates. New approach to the fracture of rubber called ''fatal agglomerate concept'' is presented. © 2008 Wiley Periodicals, Inc. J Appl Polym Sci 110: 55–60, 2008

Key words: rubber; filler agglomerates; fracture; wear; AFM; SEM; TGA; EPR

INTRODUCTION

Rubber is a multicomponent and a multiphase system. Because of generally poor mechanical properties it usually contains fillers strengthening an elastomer matrix. It is commonly accepted that the quality of filler dispersion is responsible for rubber performance. However, the degree of filler dispersion is still being evaluated on the macroscopic level,[1,2] paying less attention to the internal structure of agglomerates and aggregates. It seems likely that, depending on the morphology, fillers can exhibit different ability to stress relaxation under external deformation, e.g., faced during friction. Recent achievements of the solid-state nuclear magnetic resonance of rubber indicate on various kinds of immobilized macromolecules being present in filled systems.[3] Apart from the classical ''bound rubber''—constituting an interphase between agglomerates or aggregates and a matrix, they also originate from macromolecules infiltrating the organized filler structures. Strength of interphase interactions decides the place where the fracture of material starts from and how it propagates further. Available models describe the process of rubber wear on the macroscopic level[4] associating it with the tear strength of material. This article provides an insight into the submicron morphology of filler agglomerates and aggregates and their behavior in rubber subjected to internal stress, e.g., generated by elongation and friction. Special attention is devoted to explain the influence of rubber morphology on initiation of tear and wear of the material.

EXPERIMENTAL

Materials

Mixes of styrene–butadiene rubber (SBR; Ker 1500, ''Dworry'' S.A., Oswiqcim, Poland) filled with 50 phr of various kinds of carbon black (CB): N 110, N 234, and N 772 were prepared with a GK 50 internal mixer. Mixes of isoprene rubber (IR; Kraton IR, Shell Int., London, UK) filled with various amounts of N 772 CB were prepared with a GK 5E internal mixer. Compositions of the materials are given in Table I.

Samples were press-molded at 160°C, during time $\tau_{0.9}$ determined rheometrically according to ISO 3417. Apart from the vulcanizates before and after elongation, their wear debris and the CB used were also studied for comparison. Wear debris were collected during tribological experiments realized with a ''roll-on-plate'' T-05 apparatus (ITeE-PIB, Radom, Poland) operating under moderate loading conditions. Special attention was paid not to overheat the rubber samples subjected to wear.

Techniques

Atomic force microscopy

Surface morphology of rubber samples was studied with a Molecular Imaging Metrology Series 2000

Correspondence to: D. M. Bieliński (dbielin@p.lodz.pl).

TABLE I
Composition of the Materials Studied

Component	Symbol of rubber mix/contents (phr)						
	SBR	SBR/N110	SBR/N234	SBR/N772	IR/5 N772	IR/30 N772	IR/50 N772
Styrene butadiene rubber, Ker 1500	100	100	100	100	–	–	–
Isoprene rubber, Kraton IR-305	–	–	–	–	100	100	100
Carbon black N 110	–	50	–	–	–	–	–
Carbon black N 234	–	–	50	–	–	–	–
Carbon black N 772	–	–	–	50	5	30	50
Zinc oxide, ZnO	3	3	3	3	5	5	5
Stearic acid	1	1	1	1	2	2	2
6 PPD	2	2	2	2	–	–	–
N-Cyclohexylo-dibenzotiazolilo-sulfenamide, CBS	1.2	1.2	1.2	1.2	1	1	1
Sulfur, S_8	1.2	1.2	1.2	1.2	1	1	1

Parameters of vulcanization (ISO 3417): $T = 160°C/t = 10$ min.

(Santa Clara, CA) atomic force microscope (AFM). Samples were vulcanized against a glass plate, under optimum conditions determined rheometrically (ISO 3417), cooled down to 50°C and then separated very gently to avoid waviness of their surface layer, disabling AFM experiment. Images were collected applying either lateral force (friction) or oscillating (tapping) mode, distinguishing between the filler and the elastomer by their coefficient of friction or stiffness, respectively. Generally ''friction'' worked better for IR vulcanizates, whereas for SBR ones ''tapping'' brought good results. Commercial silicon cantilevers NSC 16 or NSC 11 (MikroMasch, Tallinn, Estonia), with the resonant frequency of 170 or 65 kHz and the force constant of 40 or 3 N/m, respectively, operating with the height and the phase scale, were used at the scan frequency of 1 Hz. AFM images were analyzed with the WS×M software,[5] enabling the fractal analysis and determination of the average distance between filler objects. Prior to the analysis pictures had been binarized, assuming the filler cut-off level being adequate to the mix composition. Fractal dimensions (*D*) of filler aggregates were calculated applying the so-called slit island algorithm.[5]

Scanning electron microscopy

Behavior of filler agglomerates under stress was analyzed with a Hitachi S-2460*N* (Tokyo, Japan) scanning electron microscope (SEM). Rubber samples, extended to relative elongations of $\varepsilon = 50$–300%, were left for resting for another 24 h. Prior to insertion into the microscope chamber the samples were covered with 10 nm of gold, applying the cathode sputtering method and a BAL-TEC SCD050 (Liechtenstein, Switzerland) apparatus, to eliminate surface charging. Images of elongated CB agglomerates were collected at magnifications ranging from 100× up to 5000×.

Thermogravimetric analysis

Experiments were performed with a Mettler Toledo STAR 851 (Columbus, OH) thermoanalytical system (TGA). Samples of $\sim$ 8–10 mg were heated with a rate of 20°/min, up to 550°C, under nitrogen atmosphere, then after changing to air, the heating was continued to 900°C. Gas flow was set to 70 mL/min. Curves of mass loss were registered. Under inert atmosphere, thermal decomposition of rubber is limited to organic components of rubber and sulfur, whereas exchanging to oxygen makes CB to decompose, which enables calculation of its content.

Electron paramagnetic resonance

Electron paramagnetic resonance (EPR) signal was determined for samples of rubber and for their wear debris with a Bruker ESP 300 (Billerica, MA) spectrometer (EPR), operating in the X band at ambient temperature. The spectrometer was equipped with precise frequency counters (Hewlett–Packard 5342A and EIP548B) (Santa Clara, CA) and with external Bruker gaussmeters (ER035M).

Experiments were carried out under the following conditions: the range of magnetic field = 30.0 mT, modulation amplitude of 0.095 mT, time constant = 80 ms, microwave power = 1 mW, and conversion time of 80 ms.

RESULTS AND DISCUSSION

Classification of filler agglomerates

AFM images of rubber vulcanizates have revealed four characteristic groups, according to the main types of the internal structure of filler agglomerates (Fig. 1):

A: infiltrated—distributive (SBR/50 phr of N 110): primary particles and small filler aggregates distributed uniformly; solid phase objects separated by continuous rubber phase.
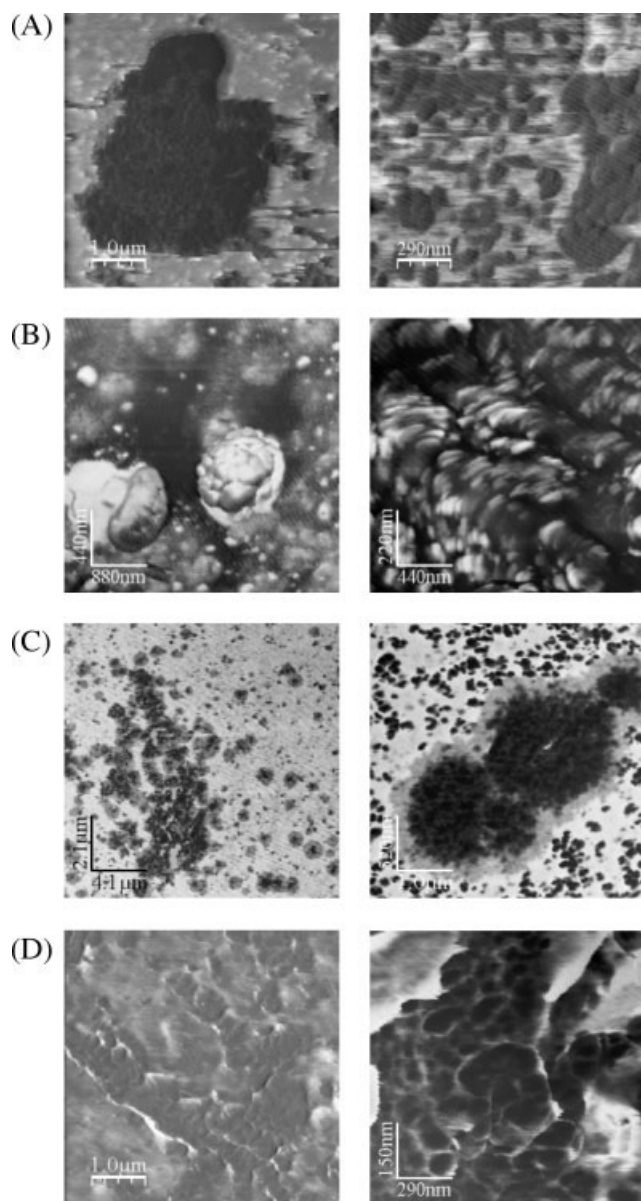
Figure 1 Classification of filler agglomerates according to their internal structure. (A) infiltrated—distributive, SBR/50 phr of N 110, (B) infiltrated—aggregative, IR/5 phr of N 772, (C) infiltrated—trapped rubber, SBR/50 phr of N 772, and (D) noninfiltrated, SBR/50 phr of N 234.

B: infiltrated—aggregative (IR/5 phr of N 772): filler aggregates of various sizes embedded in continuous rubber phase.

C: infiltrated—trapped rubber (SBR/50 phr of N 772): filler aggregates of various sizes embedded in discontinuous rubber phase.

D: noninfiltrated (SBR/50 phr of N 234): clusters of filler aggregates free of rubber phase.

Each of them exhibits different internal cohesion and adhesion to the rubber matrix. Also, thickness of the so-called bound rubber (BdR) varies from sample to sample, depending on the kind of rubber,

characteristics of CB and its amount. According to this, two kinds of bound rubber can be distinguished (Fig. 2), namely,

A—strongly immobilized and/or ''dead rubber,'' generally characteristic for vulcanizates containing active fillers (N 110 or N 234).

B—continuous BdR phase, prevailing morphology for rubber filled with ''structural filler'' (N 772).

It is likely that the main type of agglomerates present and dominating character of filler–matrix interactions decide physical properties of the rubber sample, e.g., tensile strength, wear or dynamic dumping. Neither the degree of filler dispersion nor parameters of the fractal analysis of filler agglomerates investigated extensively by many authors,[6–8] taking into account super-aggregate/agglomerate organization, seem to be important. Calculated average values of fractal parameter (D), the most representative dimension of big CB agglomerates and average interparticle distance,[9] have not reflected mechanical and tribological properties of the vulcanizates studied.

Thermogravimetric analysis

Comparison between thermographs of rubber vulcanizates and their debris indicates on changes to thermal stability of CB being present in the samples (Table II).

The temperature of 50% CB mass loss (T_{50}) is generally higher for vulcanizates in comparison to their wear debris. The difference $(\Delta T_{50} = T_{50 \text{ vulc.}} - T_{50 \text{ debris}})$ is that the higher the more active CB, the higher is
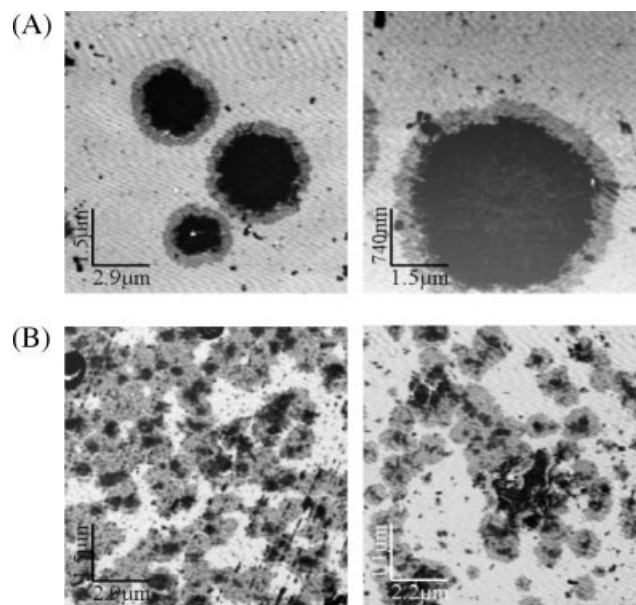
Figure 2 Classification of filler agglomerates according to their interactions with rubber matrix. (A) Strong BdR and/or ''dead'' rubber, vulcanizates containing active CB, and (B) continuous BdR, vulcanizates containing structural CB.

TABLE II
Thermal Stability of Carbon Black Being Present in
Vulcanizates and their Wear Debris

No.	Sample	T_{50} (°C)	ΔT_{50} (°C)[a]
1	IR/50 N234 vulcanizate	634	22
2	IR/50 N234 wear debris	612	
3	IR/50 N772 vulcanizate	667	13
4	IR/50 N772 wear debris	654	
5	IR/30 N772 vulcanizate	658	−6
6	IR/30 N772 wear debris	664	
7	IR/5 N772 vulcanizate	640	1
8	IR/5 N772 wear debris	639	
9	SBR/50 N110 vulcanizate	645	24
10	SBR/50 N110 wear debris	621	
11	SBR/50 N234 vulcanizate	629	13
12	SBR/50 N234 wear debris	616	
13	SBR/50 N772 vulcanizate	648	−6
14	SBR/50 N772 wear debris	654	

[a] $\Delta T_{50} = \Delta T_{50 \text{ vulc.}} - \Delta T_{50 \text{ debris}}$.

the loading. The temperature of thermooxidation of CB depends on the value of its specific surface (S).[10] The lower the S, the higher is the T_{50}, but the temperature also depends on the kind of elastomer matrix.[11] N 772 has obviously higher value of T_{50} in comparison to N 234, however, the activity of the former is higher in IR, whereas dispersion of the latter is better in SBR matrix. Reassuming, the temperature of thermal decomposition of CB can be influenced by both (1) the internal structure of filler agglomerates and filler–matrix interactions, as well as (2) the action of shearing forces accompanying friction.[12]

Fracture of rubber

According to SEM pictures of CB-filled rubber vulcanizates subjected to external stress (Fig. 3), various mechanisms of crack initiation in the material can be recognized, namely,

A: de-cohesion; B: de-adhesion; and C: simultaneous de-cohesion and de-adhesion.

Filler agglomerates generally break into smaller aggregates—vulcanizates containing N 234, which results in higher value of specific surface of CB being present in rubber debris in comparison to vulcanizates, explaining thermogravimetric data. However, in some cases the situation is reversed—usually
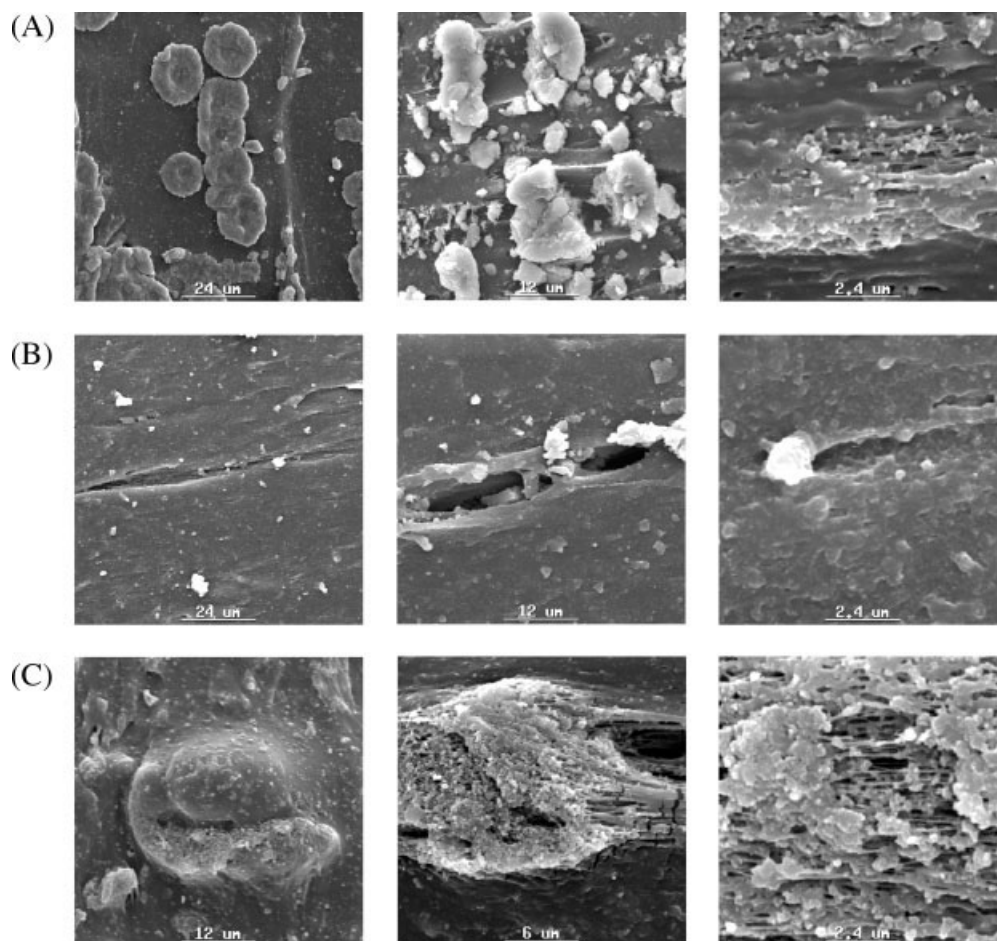
Figure 3 Behavior of filler agglomerates under tension. (A) De-cohesion, SBR/50 phr of N 234; (B) de-adhesion, SBR/50 phr of N 110, and (C) simultaneous de-cohesion and de-adhesion, SBR/50 phr of N 772.

TABLE III
Composition of Vulcanizates and their Debris Determined from TGA Spectra

No.	Sample	Average content (wt %)			
		Low molecular weight fraction	Polymer fraction	CB fraction	Mineral residues
1	IR/50 N234 vulcanizate	5.6	62.2	30.8	1.5
2	IR/50 N234 wear debris	7.6	60.2	30.6	1.7
3	IR/50 N772 vulcanizate	4.8	62.2	31.6	1.6
4	IR/50 N772 wear debris	5.9	60.8	31.6	1.7
5	IR/30 N772 vulcanizate	4.5	70.5	21.8	3.2
6	IR/30 N772 wear debris	5.7	69.2	21.7	3.3
7	IR/5 N772 vulcanizate	5.5	85.7	4.8	4.0
8	IR/5 N772 wear debris	7.2	84.0	4.9	4.0
9	SBR/50 N110 vulcanizate	2.8	63.2	32.3	1.8
10	SBR/50 N110 wear debris	3.7	62.4	31.9	1.9
11	SBR/50 N234 vulcanizate	3.2	63.8	31.5	1.5
12	SBR/50 N234 wear debris	4.0	62.9	31.3	1.8
13	SBR/50 N772 vulcanizate	2.2	63.9	32.2	1.6
14	SBR/50 N772 wear debris	2.7	63.6	32.1	1.6

very well-dispersed small aggregates of N 110, but of low interactions with rubber macromolecules crumble away from the matrix, whereas big filler structures of N 772 either breaks into smaller parts in IR matrix or deforms elastically when present in SBR one.

The morphology of rubber samples fits very well-presented interpretation of their thermogravimetric analysis and wear resistance. Wear debris contains more low-molecular weight substances than the rubber studied, as confirmed by TGA analysis (Table III). Generally higher activity of CB demands longer time for collection of debris, which is associated with higher degradation of rubber matrix. The time, however, also depends on the kind of elastomer, but only for N 234-filled systems. Degradation of rubber containing N 772 is similar, no matter IR or SBR matrix. Creation of macroradicals followed by spontaneous oxidation can also influence thermogravimetric data.

**Electron paramagnetic resonance**

The collected spectra have three types of peaks (Fig. 4), which can be assigned to

Rubber matrix: "medium" singlet (A) of peak-to peak line width $\Delta H_{PP} = 0.85$ mT and very low intensity (characteristic for unfilled SBR vulcanizates) present in the range of $g = 2.0031$. Its intensity increases more than twice for debris of unfilled vulcanizates, pointing on possible breaking of covalent bonds in rubber macromolecules, resulting from wear. It is hardly distinguishable in filled rubber spectrum, being masked by much stronger signals coming from CB.

Spins situated on the surface of filler agglomerates/aggregates: "narrow" singlet of parameters $g = 2.0024$ and $\Delta H_{PP} = 0.28$ mT found in (B) and (C)

spectra. It can be attributed to paramagnetic centers, being produced on the surface of filler due to intensive shearing. This is why it is present in the spectra of all filled samples, however being the highest for their wear debris. Rubber elongation does not influence significantly the signal.

Electrons probably situated inside filler agglomerates/aggregates: "broad" singlet occurring in (B) and (C) spectra of parameters $g = 2.0023$ and $\Delta H_{PP} \approx 7.0$ mT. The signal differs from the EPR baseline pointing on significant spin delocalization. Its intensity
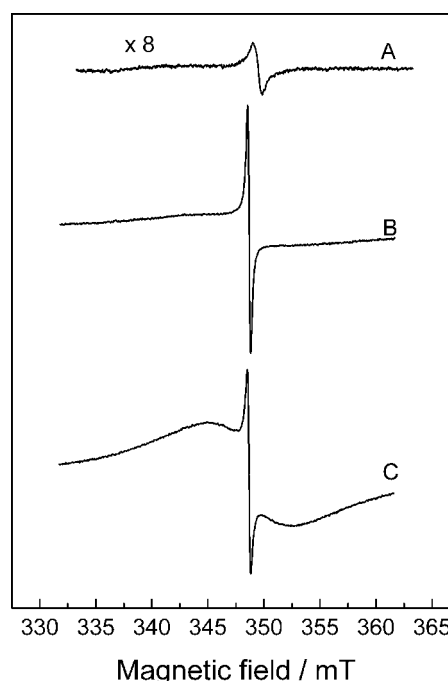
Figure 4 EPR spectra of different paramagnetic centers in (A) unfilled SBR vulcanizate, (B) debris of SBR filled with 50 phr of N 110, and (C) debris of SBR filled with 50 phr of N 772.
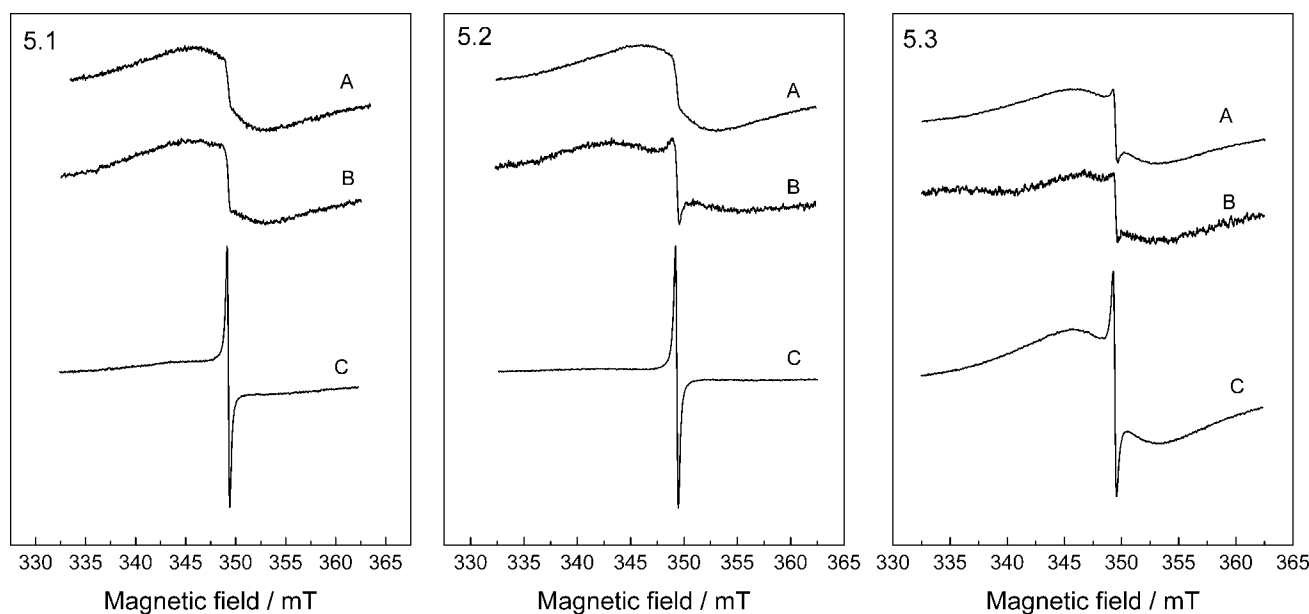
Figure 5 EPR spectra of the filled SBR vulcanizates and their debris: 5.1 containing 50 phr of N 110, 5.2 containing 50 phr of N 234, and 5.3 containing 50 phr of N 772. (A) Virgin vulcanizate, (B) SBR vulcanizate after elongation, and (C) debris of SBR vulcanizate.

is much higher in (C) than in (B) spectrum indicating that for large fillers, e.g., N 772, fraction of active centers in CB increases significantly as compared with small N 110 fillers. The results are in accordance with the expectation that upon shearing the fracture of dispersed phase composed from bigger particles proceeds more efficiently. On the other hand, in N 772 agglomerates/aggregates relative contribution of unpaired electrons situated in the border filler-vulcanizate is diminished due to smaller specific surface than in N 772.

In the EPR spectra of filled samples after elongation or in their wear debris, one can distinguish all the above peaks present in relation to the mechanism of friction initiation being involved (Fig. 5).

These results confirm our reasonable hypothesis on wear process starting from filler agglomerates, corresponding well to morphological picture and thermogravimetric data. However, as the matter of fact, origin of the signals still remains unclear. Because of wear, unpaired electrons are likely to transfer from their positions indicated as a ''broad'' singlet to others, producing a ''narrow'' one.

CONCLUSIONS

The experimental material presents more light on the structural origin of rubber fracture and wear. Despite the lack of quantitative data, already the qualitative analysis of rubber structure allows to present the hypothesis on wear being initiated either inside filler agglomerates or on the border between agglomerates

and a matrix. Taking into account the diversity of agglomerate structures, being present even within the same sample, it seems very likely that the mechanical strength and wear resistance of rubber are determined by the weakest link—the so-called fatal agglomerate. In this light, it puts under question the ''automatic'' rejection of mechanical and tribological experimental data deviating from average values suggested by standard tests procedures.

References

1. Gerspacher, M.; Nikiel, L.; Yang, H. H.; O'Farrell, C. P. Rubber Chem Technol 1997, 71, 17.
2. Bieliński, D. M.; Dobrowolski, O.; Ślusarski, L. Polimery (Warsaw) 2007, 52, 640.
3. Mansencal, R.; Haidar, B.; Vidal, A.; Delmotte, L.; Chazeau, J. M. Polymer Int 2001, 50, 387.
4. Moore, D. F. The Friction and Lubrication of Elastomers; Pergamon Press, Oxford: New York, 1972.
5. www.nanotec.es
6. Bieliński, D. M.; Dobrowolski, O.; Głąb, P.; Ślusarski L. Tribologia 2002, 184, 1081.
7. Kelbach, S.; Heinz, M.; Koglin, H. J. Kautsch Gummi Kunstst 2003, 56, 381.
8. Le, H. H.; Ilish, S.; Radusch, H.-J.; Jakob, B. Kautsch Gummi Kunstst 2003, 56, 388.
9. Bieliński, D. M.; Głąb, P.; Dobrowolski, O.; Ślusarski, L. Elastomery 2005, 9 (Special Issue), 42.
10. Jaroszyńska, D.; Kleps, T.; Tutak, D. Polimery (Warsaw) 1976, 10/11, 460.
11. Zaborski, M.; Baryń, W.; Ślusarski, L. Polimery (Warsaw) 1991, 36, 66.
12. White, J. R.; De, S. K., Eds.; Handbook of Rubber Technology; RAPRA Technology: UK, 2003; p 135.